

This discussion paper is/has been under review for the journal *Atmospheric Chemistry and Physics (ACP)*. Please refer to the corresponding final paper in *ACP* if available.

**Equatorial transport
as diagnosed from
N₂O variability**

P. Ricaud et al.

Equatorial transport as diagnosed from nitrous oxide variability

P. Ricaud¹, J.-P. Pommereau², J.-L. Attié^{1,3}, E. Le Flochmoën¹, L. El Amraoui³, H. Teyssède³, V.-H. Peuch³, W. Feng⁴, and M. P. Chipperfield⁴

¹Université de Toulouse, Laboratoire d'Aérodynamique, CNRS UMR 5560, Toulouse, France

²Service d'Aéronomie, CNRS, Verrières-Le-Buisson, France

³CNRM, Météo-France, Toulouse, France

⁴School of Earth and Environment, University of Leeds, Leeds, UK

Received: 11 December 2008 – Accepted: 2 February 2009 – Published: 24 February 2009

Correspondence to: P. Ricaud (philippe.ricaud@aero.obs-mip.fr)

Published by Copernicus Publications on behalf of the European Geosciences Union.

Title Page

Abstract

Introduction

Conclusions

References

Tables

Figures

⏪

⏩

◀

▶

Back

Close

Full Screen / Esc

Printer-friendly Version

Interactive Discussion

Abstract

The mechanisms of transport on annual, semi-annual and quasi-biennial time scales in the equatorial (10° S–10° N) stratosphere are investigated using the nitrous oxide (N₂O) measurements of the space-borne ODIN Sub-Millimetre Radiometer instrument from 5 November 2001 to June 2005, and the simulations of the three-dimensional Chemistry Transport Models MOCAGE and SLIMCAT. Both models are forced with analyses from the European Centre for Medium-range Weather Forecasts, but the vertical transport is derived either from the forcing analyses by solving the continuity equation (MOCAGE), or from diabatic heating rates using a radiation scheme (SLIMCAT). The N₂O variations 10 in the mid-to-upper stratosphere at levels above 32 hPa are shown to be generally captured by the models though significant differences appear with the observations as well as between the models, attributed to the difficulty of capturing correctly the slow vertical velocities of the Brewer-Dobson circulation. In the lower stratosphere (LS), below 32 hPa, the variations are shown to be principally seasonal with peak amplitude 15 at 400 K (~19 km), and are totally missed by the models. The decrease in diabatic radiative heating in the LS during the Northern Hemisphere summer is found to be out of phase by one month and far too small to explain the observed N₂O seasonal cycle. The proposed explanation for this annual variation is a combination of i) the annual cycle of tropopause height of 1 km amplitude, ii) the convective overshooting above 20 400 K peaking in May and absent in the models, and iii) an annual cycle of 15 ppbv amplitude of the N₂O concentration at the tropopause, but for which no confirmation exists in the upper troposphere in the absence of global-scale measurements. The present study indicates i) a significant contribution of deep convective overshooting on the chemical composition of the LS at global scale up to 500 K, ii) a preferred region for 25 that over the African continent, and iii) a maximum impact in May when the overshoot intensity is the largest and horizontal winds are the slowest.

Equatorial transport as diagnosed from N₂O variability

P. Ricaud et al.

Title Page

Abstract

Introduction

Conclusions

References

Tables

Figures

◀

▶

◀

▶

Back

Close

Full Screen / Esc

Printer-friendly Version

Interactive Discussion



1 Introduction

Nitrous oxide (N_2O) is an excellent tracer of atmospheric vertical transport since its sources are located in the troposphere (soils, wetlands, biomass burning and industrial emissions) where its lifetime is around 100 years. Its sink is in the stratosphere essentially by photolysis and reaction with electronically-excited oxygen atoms $\text{O}(^1\text{D})$, the primary source of stratospheric odd nitrogen (NO_y) (e.g. Brasseur et al., 1999), where its lifetime is less than one year. It is also a greenhouse gas and contributes to climate change (IPCC, 2001). After entering the stratosphere at the tropical tropopause, N_2O , like all long-lived species, is transported by the Brewer-Dobson circulation to high altitudes and then to the polar regions. Its spatial and temporal distribution can be thus used as a straightforward diagnostic of global-scale transport processes at different timescales, from seasons to decades.

In the mid and upper stratosphere, due to its long lifetime, the equatorial N_2O fields exhibit a strong semi-annual oscillation (SAO), as shown by Randel et al. (1994) from two years of Cryogenic Limb Array Etalon Spectrometer (CLAES) observations. This behaviour was recently confirmed by Jin et al. (2008) from the measurements of the Microwave Limb Sounder (MLS) on the AURA platform, the Atmospheric Chemistry Experiment Fourier Transform Spectrometer (ACE-FTS) and the Sub-Millimetre Radiometer (SMR) aboard ODIN. Furthermore, combining N_2O from CLAES in 1991–1993 (O’Sullivan and Dunkerton, 1997), CH_4 , and H_2O from the Halogen Occultation Experiment (HALOE) on the Upper Atmosphere Research Satellite (UARS) and O_3 from the Stratospheric Aerosol and Gas Experiment II (SAGE II) on the Earth Radiation Budget Experiment (ERBE), Randel and Wu (1996) and Baldwin et al. (2001) demonstrated the influence of the quasi-biennial oscillation (QBO) on the distribution of long-lived species in the equatorial belt.

At lower altitudes in the tropical upper troposphere-lower stratosphere (UTLS), several studies based on satellite observations of O_3 , N_2O , HCl , H_2O , HF and CH_4 from UARS/HALOE and AURA/MLS, together with ozonesondes, have shown the influence

Equatorial transport as diagnosed from N_2O variability

P. Ricaud et al.

Title Page

Abstract

Introduction

Conclusions

References

Tables

Figures

◀

▶

◀

▶

Back

Close

Full Screen / Esc

Printer-friendly Version

Interactive Discussion



**Equatorial transport
as diagnosed from
N₂O variability**P. Ricaud et al.

[Title Page](#)[Abstract](#)[Introduction](#)[Conclusions](#)[References](#)[Tables](#)[Figures](#)[I◀](#)[▶I](#)[◀](#)[▶](#)[Back](#)[Close](#)[Full Screen / Esc](#)[Printer-friendly Version](#)[Interactive Discussion](#)

of the annual oscillation (AO) and the QBO (Randel et al., 2007; Schoeberl et al., 2008), whilst Gettelman et al. (2004) explored the impact of the monsoon during the June–August period. Finally, Ricaud et al. (2007) from a combination of ODIN N₂O, HALOE CH₄ and MLS CO observations have shown the large variations of species concentrations in the equatorial low stratosphere in March–April–May (MAM), displaying marked maxima over Africa and other land areas, very consistent with the overshooting picture derived from the Tropical Rainfall Measuring Mission (TRMM) Precipitation Radar.

As an extension of the previous study, here we investigate how N₂O behaves in the entire equatorial stratosphere including the Tropical Tropopause Layer (TTL) over a five year time period by combining ODIN/SMR measurements from 2001 to 2006 and long-term runs of the three-dimensional (3-D) chemical transport models (CTMs) SLIMCAT and MOCAGE. Particular attention will be paid to the UTLS to see how the contrast between land and oceanic regions observed by Ricaud et al. (2007) in MAM 2002–2004, extends to other seasons.

Information on the ODIN N₂O observations and model simulations are provided in Sect. 2. Section 3 is devoted to the presentation of the time evolution of N₂O in the stratosphere from November 2001 to June 2005 in the equatorial belt and the influence of annual, semi-annual and quasi-biennial oscillations. Section 4 concentrates on the annual oscillation in the lower stratosphere and its possible explanations. Section 5 summarises our findings.

2 Observations and models

2.1 ODIN

The data used here are from the ODIN/SMR instrument. The ODIN mini-satellite (Murtagh et al., 2002) was placed into a 600-km sun-synchronous, terminator orbit in February 2001 and is still operational. The platform includes the SMR microwave instrument (Frisk et al., 2003) that can measure O₃, ClO, N₂O, HNO₃, H₂O, and CO in

**Equatorial transport
as diagnosed from
N₂O variability**P. Ricaud et al.

[Title Page](#)[Abstract](#)[Introduction](#)[Conclusions](#)[References](#)[Tables](#)[Figures](#)[◀](#)[▶](#)[◀](#)[▶](#)[Back](#)[Close](#)[Full Screen / Esc](#)[Printer-friendly Version](#)[Interactive Discussion](#)

the frequency domain 480–580 GHz, most of its measurements being validated (e.g. Barret et al., 2006). The present study is based on the retrievals of the 502.296-GHz N₂O line using the Optimal Estimation Method (Rodgers, 2000). On average, N₂O measurements are performed one day out of three, due to sharing of the instrument with astronomy. All measurements performed between November 2001 and July 2005 have been analyzed using version V222 of the retrieval algorithm (Urban et al., 2005). Note that from November 2005 to October 2006, ODIN N₂O data has been processed using version V225 of the retrieval algorithm but this data is not used in the present analysis that only covers November 2001–June 2005. The vertical resolution is 2 km. The single-scan precision ranges from 10 to 45 ppbv for N₂O mixing ratios varying from 0 to 325 ppbv. The total systematic error varies from 3 to 35 ppbv for N₂O mixing ratios from 0 to >150 ppbv. In the UTLS, the single scan precision is ~39 and ~24 ppbv (~10–12%) at 100 hPa and 70 hPa, respectively and the total systematic error is ~22 and ~13 ppbv (~4–6%), respectively. All measurements have been averaged into bins of 10° latitude×30° longitude.

2.2 SLIMCAT

SLIMCAT is an off-line 3-D CTM described in detail in Chipperfield (1999). The model uses a hybrid σ – θ vertical coordinate and extends from the surface to a top level which depends on the domain of the forcing analyses. Vertical advection in the θ -level domain (above 350 K) is calculated from diabatic heating rates using a radiation scheme which gives a better representation of vertical transport and age-of-air even with European Centre for Medium-range Weather Forecasts (ECMWF) ERA40 analyses than using vertical winds derived from the analyses which have known problems (Chipperfield, 2006). The model contains a detailed stratospheric chemistry scheme. The present experimental set up is detailed in Feng et al. (2007). The horizontal resolution is 7.5°×7.5° with 24 levels from the surface to about 60 km. The model was forced using the 6-hourly 60-level ECMWF analyses from January 1977 to June 2005. From 1 January 1977 to 31 December 2001 the standard ERA-40 product is used (Uppala

et al., 2005), and after this date, the operational analyses are employed. In the run used here there is no explicit treatment of tropospheric convection. The troposphere is assumed well mixed, i.e. tropospheric trace gases are mixed with a constant volume mixing ratio profile up to the tropopause (380 K in the tropics). The time evolution of surface mixing ratios of greenhouse gases (particularly N_2O) is prescribed according to the Intergovernmental Panel on Climate Change (IPCC) recommendations (IPCC, 2001). Furthermore, the model run covers the period 1977–2005 for studying the long-term evolution of N_2O but only equatorial (10°S – 10°N) zonally-averaged N_2O data from November 2001 to June 2005 are used in the present study.

2.3 MOCAGE

MOCAGE-Climat (Teyssède et al., 2007) is the climate version of Météo-France's tropospheric-stratospheric MOCAGE 3-D CTM. The climate version used in this study has 60 layers from the surface up to 0.07 hPa, with a horizontal resolution of $5.6^\circ \times 5.6^\circ$. ECMWF 6-hourly analyses were used to force the model from 1 January 2000 to 31 December 2005. MOCAGE uses a semi-Lagrangian advection scheme and vertical velocities are recalculated from the forcing analyses by solving continuity equation. MOCAGE-Climat contains a detailed tropospheric-stratospheric chemistry scheme. Initial chemical conditions were taken from a previous simulation to allow the model to quickly reach its numerical equilibrium, especially for long-lived species, such as N_2O . Surface emissions prescribed in MOCAGE-Climat are based upon yearly- or monthly-averaged climatology. The N_2O surface emissions are taken from the Global Emissions Inventory Activity and are climatology representative of the year 1990 (Bouwman et al., 1995). They include anthropogenic and biogenic sources, for a total emission rate of $14.7\text{ Tg(N) yr}^{-1}$. Note that, regarding convection, the present run was performed using the scheme of Betchold et al. (2001). Modelled data have been averaged into bins of 10° latitude \times 30° longitude and used over the period November 2001–June 2005. More information can be found in Ricaud et al. (2007).

Equatorial transport as diagnosed from N_2O variability

P. Ricaud et al.

Title Page

Abstract

Introduction

Conclusions

References

Tables

Figures

◀

▶

◀

▶

Back

Close

Full Screen / Esc

Printer-friendly Version

Interactive Discussion



3 Influence of transport on the N₂O stratospheric distribution

The N₂O anomaly (defined as the difference between the N₂O field and its mean and linear trend over the period) in the ODIN, MOCAGE and SLIMCAT data sets during the period 2000–2006 from 100 to 1 hPa is shown in Fig. 1, onto which the ECMWF zonal wind u is superimposed. Easterlies (westerlies) are represented by solid (dashed) lines. The vertical distributions of the amplitude of the AO, SAO and QBO during the November 2001–June 2005 overlapping period derived from these data are shown in Fig. 2 as a function of pressure. The correlation coefficients between N₂O concentrations and ECMWF zonal and vertical winds calculated from the integration of the mass-conservative continuity equation are displayed in Tables 1 and 2, respectively.

3.1 Mid-to-upper stratosphere (32–1 hPa)

In the mid-to-upper stratosphere, the three oscillations (AO, SAO and QBO) compete in the ODIN observations, the AO and SAO dominating in the upper stratosphere (5–1 hPa) and the QBO in the middle stratosphere (32–5 hPa). A strong AO signal is seen from 22 to 1 hPa with a broad maximum at around 4.6 hPa of ~15 ppbv. As shown by Schoeberl et al. (2008), the AO signal results from the annual variation of the vertical velocity in the lower stratosphere. The correlation r between N₂O and vertical winds is moderately high, i.e. 0.53–0.66 between 21–2.1 hPa.

A strong SAO signal is observed in the upper stratosphere with marked positive anomalies occurring every two years in 2002, 2004 and 2006. As already noted by Schoeberl et al. (2008) and Jin et al. (2008), the positive (negative) anomalies in the upper stratosphere SAO cycle are in phase with westerly (easterly) QBO phases in the middle stratosphere. The SAO contribution is significant from 10 to 1.5 hPa with a maximum of about 15 ppbv at 4.6 hPa.

A QBO signal also appears in the middle stratosphere with a downward propagation of positive (negative) N₂O anomalies associated with easterly (westerly) phases. The QBO cycle is known to originate in the momentum deposition produced by the damp-

Title Page

Abstract

Introduction

Conclusions

References

Tables

Figures

◀

▶

◀

▶

Back

Close

Full Screen / Esc

Printer-friendly Version

Interactive Discussion



Equatorial transport as diagnosed from N₂O variability

P. Ricaud et al.

Title Page

Abstract

Introduction

Conclusions

References

Tables

Figures

◀

▶

◀

▶

Back

Close

Full Screen / Esc

Printer-friendly Version

Interactive Discussion

ing in the stratosphere of several waves (Rossby, Kelvin, gravity waves, etc.), excited by diabatic thermal process in the troposphere (e.g. Cariolle et al., 1993). The QBO easterly (westerly) phase at 40 hPa is associated with an upward (downward) mean meridional circulation bringing N₂O-rich (-poor) air upward (downward). Since easterlies are stronger and last longer than westerlies, the positive N₂O anomaly in the data also lasts longer than the negative anomaly with a downward propagation from 4.6 to 21 hPa consistent with model calculations of 1 km month⁻¹. Around 20–30 hPa and below, the westerly wind regime propagates downward at constant velocity with little variation between cycles, whilst the descent speed of easterlies slows down at lower altitude (Kinnersley and Pawson, 1996). Because of the stalling of easterlies, the time between maximum easterlies and maximum westerlies is much shorter than the reverse (Naujokat, 1986). This explains the asymmetric descent rates of easterly and westerly regimes seen in the N₂O concentration with positive anomalies lasting longer than negative ones in the lower stratosphere. The QBO signal extends from 32 to 1 hPa with a maximum amplitude of ~20 ppbv peaking at 10 hPa. The anti-correlation r between N₂O data and zonal winds is indeed very high (0.60–0.74) between 21 and 1 hPa.

The two CTMs globally match the data above 32 hPa to within ±5 ppbv as well as the amplitude of the AO, SAO and QBO signals (Fig. 2), in contrast to the CMAM chemistry-climate model (Jin et al., 2008), which cannot capture the QBO structure. Nevertheless, some significant differences with the observations are also apparent. The SLIMCAT AO signal is consistent with that of ODIN, but MOCAGE underestimates its amplitude by 5–10 ppbv between 2.2 and 6.8 hPa. The SLIMCAT SAO is 10–15 ppbv larger than that observed between 2.2 and 4.6 hPa, which is better matched by MOCAGE. Finally, the QBO is very well reproduced by MOCAGE, whereas SLIMCAT underestimates its amplitude by 10–15 ppbv between 10 and 20 hPa.

However, most remarkable (Fig. 2) is the amplitude of the differences between the two models of the same order of magnitude as those between models and observations. Although the slightly different horizontal resolution between the two (7.5° × 7.5° for

SLIMCAT and $5.6^\circ \times 5.6^\circ$ for MOCAGE) may contribute, the major difference likely results in their method for calculating the vertical advection, forced by ECMWF analyses in MOCAGE and derived from diabatic heating rates in SLIMCAT. The anti-correlation between N_2O and zonal winds (Table 1) is indeed very high (0.55–0.75) in MOCAGE and SLIMCAT between 10 and 1 hPa, as observed. However, the correlation between N_2O and vertical winds (Table 2) between 2.1 and 10 hPa is rather poor in SLIMCAT (0.22–0.50) whilst in MOCAGE the correlation is greater (0.37–0.59) and somewhat more consistent, although smaller, with the ODIN values (0.53–0.56). Once again, this illustrates the importance of vertical advection in the control of the vertical distribution of chemical species in the stratosphere, but also the difficulty of reproducing these small vertical velocities in models.

3.2 UTLS (100–32 hPa)

At altitudes below 32 hPa, the AO dominates in the observations, except at 100 hPa where a SAO signal of similar magnitude can be seen. Compared to this, the AO is almost missing in the models, while both the SAO and the QBO are underestimated in the TTL at levels below 68 hPa. In contrast with the models displaying correlation between N_2O concentration and ECMWF vertical advection (0.69 in SLIMCAT at 100 hPa, and 0.61 in MOCAGE at 46 hPa), the observed variations are totally disconnected from these. The inability of the models to reproduce observations suggests that other mechanisms, not currently included or poorly treated in the model schemes, are controlling the N_2O cycle at these levels.

4 Annual oscillation in the UTLS

To explore the possible reasons for the large AO signal in the observations below 32 hPa, which is missed by the models, the N_2O mean seasonal variations have been investigated in more detail. Figure 3 displays the seasonal variation of observed and

Equatorial transport as diagnosed from N_2O variability

P. Ricaud et al.

Title Page

Abstract

Introduction

Conclusions

References

Tables

Figures

◀

▶

◀

▶

Back

Close

Full Screen / Esc

Printer-friendly Version

Interactive Discussion



**Equatorial transport
as diagnosed from
N₂O variability**P. Ricaud et al.

[Title Page](#)[Abstract](#)[Introduction](#)[Conclusions](#)[References](#)[Tables](#)[Figures](#)[◀](#)[▶](#)[◀](#)[▶](#)[Back](#)[Close](#)[Full Screen / Esc](#)[Printer-friendly Version](#)[Interactive Discussion](#)

modelled monthly mean N₂O concentration at 100, 68, 46 and 32 hPa, the levels of the ODIN/SMR measurements, averaged between November 2001 and June 2005. To identify possible geographic differences in the observations reported by Ricaud et al. (2007), also shown are the mean concentrations over the African (30° W–60° E) and the Western Pacific (120° E–150° W) sectors. To subtract the contribution of the well-known seasonal cycle of isentropic surface height on which the mixing ratio would remain constant if no diabatic vertical transport was involved, the N₂O fields have been linearly interpolated on potential temperature surfaces. Figure 4 shows the seasonal variations of N₂O fields interpolated at 400, 450, 500 and 550 K and Fig. 5 displays the contrast between African and Western Pacific sectors. Figure 6 shows the seasonal cycles of NCEP tropopause temperature and pressure, upwelling from thermodynamic balance from Randel et al. (2007), and potential temperature changes between 15–23 km. A minimum height and maximum temperature of the tropopause, and a maximum potential temperature at levels above peaking at 19 km is observed in August, while the minimum upwelling occurs one month earlier.

4.1 Seasonal cycle

A seasonal cycle is observed in the ODIN zonal mean (black dots) at all levels with a minimum from May to August at 100 hPa (~16.5 km) or 400 K (~18 km), extending to September at higher altitude. Its amplitude is a maximum at 68 hPa and 400 K. The minimum N₂O in June is consistent with that derived by Jin et al. (2008) from the same ODIN observations (using the Swedish algorithm version 2.1 from July 2001 to February 2007), as well as from AURA/MLS, although the broader MLS vertical resolution results in a weaker contrast. A small semi-annual oscillation (secondary minimum in January) can also be seen at 100 hPa in Fig. 3, but disappears in the potential temperature plots in Fig. 4, suggesting an influence of the tropopause height.

There is no time lag between the minimum which always occurs in June at all altitudes up to 550 K (22.5 km) or 32 hPa (24 km), that is no indication of a tape-recorder type signature such has seen in the HALOE water vapour at higher altitudes, mean-

**Equatorial transport
as diagnosed from
N₂O variability**

P. Ricaud et al.

[Title Page](#)[Abstract](#)[Introduction](#)[Conclusions](#)[References](#)[Tables](#)[Figures](#)[⏪](#)[⏩](#)[◀](#)[▶](#)[Back](#)[Close](#)[Full Screen / Esc](#)[Printer-friendly Version](#)[Interactive Discussion](#)

ing that the minimum propagates upward far faster than the $0.2\text{--}0.3\text{ km month}^{-1}$ of the Brewer-Dobson circulation (Mote et al., 1996). The absence of N₂O phase shift with altitude in the lower stratosphere was also noticed by Schoeberl et al. (2008) in the MLS data, and was attributed to the signature to the seasonal variation of the Brewer-Dobson upward velocity. However, since the minimum N₂O is observed in June, one month in advance relative to the minimum upward velocity in July (Randel et al., 2007 and Fig. 6), there is a contradiction which is difficult to reconcile.

However, most important for understanding the mechanism responsible for the AO is the contrast between the Western Pacific and the African sectors being maximum in May–July at 100 hPa (16.5 km) and at 400 K (18 km), and insignificant above, except in May (Fig. 5). The amplitude of the seasonal cycle is smaller above Africa than above the Western Pacific at 100 hPa and at 400 K.

Compared to the observations, the two models show little seasonal variation. SLIMCAT displays a slight minimum in August–September of small amplitude consistent with the known minimum diabatic radiative heating in July–August (e.g. Randel et al., 2007 and Fig. 6), shifted by 1 month because of the slow ascent rate of $600\text{--}800\text{ m month}^{-1}$. Given the assumed well mixed troposphere in SLIMCAT, this annual cycle reflects the varying altitude of the model tropopause. MOCAGE also shows almost no seasonal variation but the well-known ECMWF too fast ascent of the Brewer-Dobson circulation above 21 km (Monge-Sanz et al., 2007, and references therein). The same applies to the CMAM model which underestimates the amplitude of the minimum N₂O shifted also to August–September (Jin et al., 2008). In summary, the N₂O seasonal cycle in the TTL and lower stratosphere reported by ODIN requires mechanisms which do not exist in the currently available CTM global models.

4.2 Discussion

The question is thus: what could be these mechanisms?

4.2.1 Possible contributions

Ignoring here the specific issue of water vapour which involves still unresolved questions of hydration-dehydration processes, the presence of a seasonal cycle in the concentration of several tropospheric tracers, as well as ozone, in the tropical UTLS has been already noted by Folkins et al. (2006), Randel et al. (2007), Jin et al. (2008), and Schoeberl et al. (2008). The AO is generally attributed to the seasonal cycle of the vertical velocity of the diabatic heating and the Brewer-Dobson circulation. However, there are differences in the phase of the AO between the species difficult to reconcile with a minimum vertical velocity in July. An ozone maximum and a carbon monoxide minimum are observed in August (Randel et al., 2007) peaking at about 17.5 km and 100 hPa, respectively and, from the present study, a minimum N₂O occurs in June at 18–19 km propagating to 21–22 km with no phase shift, one-month ahead the minimum in upwelling in July.

Several mechanisms could contribute to the AO whose impacts will depend on the lifetime and on the vertical distribution of the species. The first is the vertical transport of the species by diabatic heating or height displacement of the tropopause and isentropic surfaces immediately above, both displaying a seasonal cycle but shifted by one month (Fig. 6). The amplitude of the variation of concentration of the species at a given altitude or pressure level will depend on its vertical gradient at this level. It will be large for ozone for which a vertical displacement of only 250 m within a vertical gradient of 0.8 ppmv km⁻¹ could explain the 0.15 ppmv amplitude of the AO at 17.5 km seen by Randel et al. (2007). It will be smaller for CO for which the same displacement within a vertical gradient of -14 ppbv km⁻¹ will result in a change of 3.5 ppbv only at 17.5 km. It will be very small for N₂O since a vertical gradient of -6 ppbv km⁻¹ will only produce a 1.5 ppbv change in the lower stratosphere.

The second important parameter is the lifetime of the species in the lower stratosphere. The 2-month chemical lifetime of CO implies that its concentration decreases rapidly with time compared to the O₃ and N₂O long-lived species for which the change

Equatorial transport as diagnosed from N₂O variability

P. Ricaud et al.

Title Page

Abstract

Introduction

Conclusions

References

Tables

Figures

◀

▶

◀

▶

Back

Close

Full Screen / Esc

Printer-friendly Version

Interactive Discussion



within one year is negligible.

The third contributing parameter is the seasonal cycle of the species in the upper troposphere (UT) resulting from variations of surface source emissions, chemical processes (e.g. lightning NO_x) and convective lifting. In the case ozone, the seasonal change in the tropical UT is limited to 30–40 ppbv maximum at 15 km (Randel et al. 2007). The CO variation at 147 hPa shows a small (5 ppbv) AO but a larger SAO of 25 ppbv amplitude with minima in December–February and July–September (Randel et al., 2007). Unfortunately there is little information on N_2O in the UT, only recent indications from the nadir-viewing Infrared Atmospheric Sounding Interferometer (IASI) aboard MetOp-A of a maximum total column (mainly in the mid-troposphere) in the equatorial belt in MAM 2008 over Africa (Ricaud et al., 2008).

The fourth and last potential contributor to an AO cycle is the fast convective overshooting of tropospheric air above continental regions and particularly Africa, between February and May and, to a lesser extent, in September–November as shown by the overshooting volume in the 10°S – 10°N band (Fig. 7) derived from the TRMM precipitation radar overshooting features (Liu and Zipser, 2005). This mechanism was that suggested by Ricaud et al. (2007) for explaining the contrast in N_2O , CH_4 and CO concentrations in the lower stratosphere between the Western Pacific, Africa and other continental areas. However, the amplitude of the contrast between various regions will also depend on the zonal wind velocity that is the time needed for local injections in preferred regions to mix up at zonal scale. The seasonal cycle of each species will be a combination of all these parameters whose impacts will depend on the specific characteristics of each species.

4.2.2 Ozone

Because of its maximum vertical gradient at 17.5 km, the ozone AO (Randel et al., 2007) is dominated by the signature of the annual cycle of the vertical displacement, although convective overshooting could also contribute as shown by the small differences between the different Southern Hemisphere Additional Ozonesondes (SHADOZ)

Equatorial transport as diagnosed from N_2O variability

P. Ricaud et al.

Title Page

Abstract

Introduction

Conclusions

References

Tables

Figures

⏪

⏩

◀

▶

Back

Close

Full Screen / Esc

Printer-friendly Version

Interactive Discussion



stations during the period of minimum ozone in February–March. A vertical displacement of 250 m in the 0.8 ppmv km^{-1} vertical gradient will be enough to explain the 0.15 ppmv amplitude of the cycle. The very limited AO amplitude at 20 km suggests that the main process responsible could be the seasonal variation of isentropic surface heights of rapidly decreasing amplitude with altitude above the tropopause.

From Fig. 6, if we consider the two time distributions of the tropopause pressure and of the upwelling, although both of them are peaking in July, the minimum of the distribution is located end of July for the upwelling and mid of August for the tropopause pressure. The ozone and tropopause pressure cycles are thus perfectly in phase, in contrast with the one-month shift of the ascent by radiative heating which would require only 10 days for a 250 m displacement.

4.2.3 Carbon monoxide

The CO seasonal cycle at 68 hPa (19 km) (Randel et al., 2007) shows a minimum in September–November shifted by 2–3 months compared to the radiative ascent rate, followed by a fast increase in November–December and a maximum in February–March. Since a vertical displacement, either radiative ascent or isentropic surface lift, will have a limited impact on the concentration of the species, the observations will be better compatible with overshooting during the convective season in February–May, followed by a 40% photochemical reduction during the following 5 months. Overshoot episodes, such as those reported by Ricaud et al. (2007), could also explain the fast anti-correlated CO–O₃ changes of up to 8 ppbv CO amplitude observed in the winter within less than 15 days, which would require vertical velocity variations of more 0.6 mm s^{-1} ($1.5 \text{ km month}^{-1}$, 1 K day^{-1}) difficult to reconcile with radiative heating calculation (Folkins et al., 2006; Corti et al., 2005).

Equatorial transport as diagnosed from N₂O variability

P. Ricaud et al.

Title Page

Abstract

Introduction

Conclusions

References

Tables

Figures

◀

▶

◀

▶

Back

Close

Full Screen / Esc

Printer-friendly Version

Interactive Discussion



4.2.4 Nitrous oxide

N_2O (Fig. 3) displays a zonal mean seasonal cycle of 15 ppbv amplitude at 100 hPa, increasing to 20 ppbv at 68 hPa (19 km), and then reducing progressively at higher altitude, with a minimum in May–July. Within an average -6 ppbv km^{-1} vertical gradient as observed by ODIN at least above 68 hPa, this would correspond to a vertical displacement of 2.5, 3.3, 2.0 and 1.7 km at 100, 68, 46 and 32 hPa, respectively. After interpolation on isentropic surfaces for correcting for the seasonal variation of the isentropic surface height (Fig. 4), the amplitude is slightly reduced by 1–3 ppbv. The main consequence is the reduction of the September–October maximum at 400 K and that of November–December at 450 K and thus the removal of the SAO signal. However, most apparent is the larger amplitude of the cycle above the Western Pacific (19 ppbv) than over Africa (14 ppbv) at 400 K (Fig. 5), the contrast being maximum (12 ppbv) in May. Except in May, this contrast vanishes at higher altitude.

Since the minimum N_2O occurs one month before the drop in the upwelling calculated from thermodynamic balance (Randel et al., 2007) and since its amplitude would imply a relative subsidence of -1.1 mm s^{-1} (-1.9 K day^{-1}) in contradiction with all calculations (Folkins et al., 2006; Corti et al., 2005), the N_2O seasonal cycle cannot be explained by the modulation of the vertical transport by radiative heating. Instead, the peak contrast between the Western Pacific and Africa in May up to 500 K (21 km) coincident with that of the maximum overshooting volume derived from the TRMM observations, suggests a clear contribution of deep convective overshooting combined with a small horizontal mixing during the period of minimum zonal wind (Fig. 8).

However, this process alone should result in an increase of the N_2O concentration and not the opposite; something else is required. Figure 9 shows the seasonal change of the ODIN N_2O vertical profile as well as those of the models. The strong gradient reduction at all levels below 500 K starting in January, reaching a maximum in May compared to the following months, confirms the injection of tropospheric air up to this altitude and particularly over Africa. As expected, the models completely miss

Equatorial transport as diagnosed from N_2O variability

P. Ricaud et al.

Title Page

Abstract

Introduction

Conclusions

References

Tables

Figures

◀

▶

◀

▶

Back

Close

Full Screen / Esc

Printer-friendly Version

Interactive Discussion



those changes, MOCAGE showing too fast vertical transport almost constant throughout the year and SLIMCAT, based on radiative calculations, slower average velocity with a slight minimum in August–September.

However, the picture also shows that the May–August minimum concentration originates at the bottom of the profile, at the tropopause, implying a large seasonal change in the UT. Unfortunately, apart from the recent IASI total columns consistent with the ODIN indications at 100 hPa (Ricaud et al., 2008), there is no N₂O measurement available in the UT to confirm unambiguously the hypothesis. MOCAGE (Fig. 10) displays a maximum in NDJ associated to convective activity over Africa, consistent with ODIN, but of only 1.5 ppbv amplitude instead of the observed 15 ppbv. However, since seasonal changes in the surface sources and overshooting are ignored in the model, this is of limited significance.

In summary, the observed ODIN N₂O seasonal cycle in the lower stratosphere, different to those of O₃ and CO, and the contrast of concentration between the Western Pacific and the African sectors, would be the result of a minimum N₂O concentration in the upper troposphere in May–July and deep convective overshooting in February–May combined with a minimum horizontal mixing in May–June.

The above findings fully confirm the hypothesis of the convective origin of the larger N₂O concentration over Africa than over the Western Pacific during the March–May period reported earlier by Ricaud et al. (2007) and thus the significant contribution of convective overshooting on the chemical composition of the lower stratosphere at global scale up to 20–21 km altitude.

5 Conclusions

The evolution of the concentration of the long-lived N₂O species in the stratosphere has been studied from the measurements of the space-borne ODIN/SMR instrument from November 2001 to June 2005. The mechanisms responsible for the observed oscillations have been explored by confronting the measurements to simulations of

Equatorial transport as diagnosed from N₂O variability

P. Ricaud et al.

Title Page

Abstract

Introduction

Conclusions

References

Tables

Figures

⏪

⏩

◀

▶

Back

Close

Full Screen / Esc

Printer-friendly Version

Interactive Discussion



two chemistry transport models (CTMs), both forced with ECMWF analyses, whilst the vertical transport is derived from the forcing analyses by solving the continuity equation (MOCAGE) and from diabatic heating rates using a radiation scheme (SLIMCAT).

The observed N₂O variations are found to be influenced by the annual, semi-annual and quasi-biennial oscillations of comparable amplitudes in the mid-stratosphere, whilst the AO dominates below 32 hPa with amplitude peaking at 68 hPa, and a significant SAO signature at 100 hPa. Both CTMs generally match the data above 32 hPa to within ±5 ppbv as well as the amplitude of the AO, SAO and QBO signals. However, significant differences appear with the observations as well as between the models, attributed to the difficulty of capturing correctly the slow vertical velocities of the Brewer-Dobson circulation.

The situation is worse in the lower stratosphere where the models, although one of them includes radiative heating, totally miss the annual oscillation. The drop of diabatic radiative heating during the Northern Hemisphere summer in July is found to be out of phase by one month and far too small for explaining the observations. The processes involved are shown to be a combination of the annual variation of tropopause height of 1 km amplitude, convective overshooting up to 500 K totally ignored in the models, and an annual cycle of 15 ppbv amplitude of the N₂O concentration observed at the tropopause, but for which there is still little confirmation in the upper troposphere in the absence of global-scale profile measurements. The larger N₂O concentration in the lower stratosphere over Africa compared to the Western Pacific during the convective period reported by Ricaud et al. (2007) is fully confirmed. The most important implication of the findings is the demonstration of the significant contribution of convective overshooting on the chemical composition of the lower stratosphere at the global scale up to 500 K (20–21 km).

Acknowledgements. Odin V222 data have been obtained from the ETHER French atmospheric database (<http://ether.ipsl.jussieu.fr>). The project was funded by the French CNRS-INSU-CNES LEFE programme, the SCOUT-O3 and ACCENT AT2 projects of the European Commission which are gratefully acknowledged. The SLIMCAT modelling was supported by NERC

Equatorial transport as diagnosed from N₂O variability

P. Ricaud et al.

Title Page

Abstract

Introduction

Conclusions

References

Tables

Figures

◀

▶

◀

▶

Back

Close

Full Screen / Esc

Printer-friendly Version

Interactive Discussion



The publication of this article is financed by CNRS-INSU.

5 References

- Baldwin, M. P., Gray, L. J., Dunkerton, T. J., et al.: The quasi-biennial oscillation, *Rev. Geophys.*, 39, 179–229, 2001.
- Barret, B., Ricaud, P., Santee, M. L., et al.: Intercomparisons of trace gases profiles from the Odin/SMR and Aura/MLS limb sounders, *J. Geophys. Res.*, 111, D21302, doi:10.1029/2006JD007305, 2006.
- Betchold, P., Bazile, E., Guichard, F., et al.: A mass flux convection scheme for regional and global models, *Q. J. Roy. Meteor. Soc.*, 127, 869–886, 2001.
- Bouwman, A. F., Van der Hoek, K. W., and Olivier, J. G. J.: Uncertainties in the global source distribution of nitrous oxide, *J. Geophys. Res.*, 100(D2), 2785–2800, 1995.
- Brasseur, G., P., Orlando, J. J., and Tyndall, G. S.: *Atmospheric Chemistry and Global Change*, 2nd edn., Oxford University Press, New York, Oxford, ISBN-0-19-510521-4, 1999.
- Cariolle, D., Amodei, M., Déqué, M., et al.: A quasi-biennial oscillation signal in general circulation model simulations, *Science*, 261, 1313–1316, 1993.
- Chipperfield, M. P.: Multiannual simulations with a three-dimensional chemical transport model, *J. Geophys. Res.*, 104, 1781–1805, 1999.
- Chipperfield, M. P.: New version of the TOMCAT/SLIMCAT offline chemical transport model: intercomparison of stratospheric tracer experiments, *Q. J. Roy. Meteor. Soc.*, 132, 1179–1203, doi:10.1256/qj.05.51, 2006.
- Corti, T., Luo, B. P., Peter, P., Vömel, H., and Fu, Q.: Mean radiative energy balance and vertical

Equatorial transport as diagnosed from N₂O variability

P. Ricaud et al.

Title Page

Abstract

Introduction

Conclusions

References

Tables

Figures

◀

▶

◀

▶

Back

Close

Full Screen / Esc

Printer-friendly Version

Interactive Discussion



**Equatorial transport
as diagnosed from
N₂O variability**

P. Ricaud et al.

[Title Page](#)[Abstract](#)[Introduction](#)[Conclusions](#)[References](#)[Tables](#)[Figures](#)[◀](#)[▶](#)[◀](#)[▶](#)[Back](#)[Close](#)[Full Screen / Esc](#)[Printer-friendly Version](#)[Interactive Discussion](#)

mass fluxes in the equatorial upper troposphere and lower stratosphere, *Geophys. Res. Lett.*, 32, L06802, doi:10.1029/2004GL021889, 2005.

Feng, W., Chipperfield, M. P., Dorf, M., et al.: Mid-latitude ozone changes: studies with a 3-D CTM forced by ERA-40 analyses, *Atmos. Chem. Phys.*, 7, 2357–2369, 2007, <http://www.atmos-chem-phys.net/7/2357/2007/>.

Folkens, I., Bernath, P., Boone, C., Lesins, G., Livesey, N., Thompson, A. M., Walker, K., and Witte, J. C.: Seasonal cycles of O₃, CO and convective outflow at the tropical tropopause, *Geophys. Res. Lett.*, 33, L16802, doi:10.1029/2006GL026602, 2006.

Frisk, U., Hagström, M., Ala-Laurinaho, J., et al.: The Odin satellite I: Radiometer design and test, *Astron. Astrophys.*, 402, L27–L34, doi:10.1051/0004 6361:20030335, 2003.

Gettelman, A., Kinnison, D. E., Dunkerton, T. J., and Brasseur, G. P.: Impact of monsoon circulations on the upper troposphere and lower stratosphere, *J. Geophys. Res.*, 109, D22101, doi:10.1029/2004JD004878, 2004.

Intergovernmental Panel on Climate Change: Climate change 2001: The scientific basis, contribution of working group I to the third Assessment report of the IPCC, edited by Houghton, J. T. et al., Cambridge Univ. Press, New York, 2001.

Jin, J. J., Semeniuk, K., Beagley, S. R., et al.: Comparison of CMAM simulations of carbon monoxide (CO), nitrous oxide (N₂O), and methane (CH₄) with observations from Odin/SMR, ACE-FTS, and AURA/MLS, *Atmos. Chem. Phys. Discuss.*, 8, 13063–13123, 2008, <http://www.atmos-chem-phys-discuss.net/8/13063/2008/>.

Kinnersley, J. S. and Pawson, S.: The descent rates of the shear zones of the equatorial QBO, *J. Atmos. Sci.*, 53, 1937–1949, 1996.

Liu, C. and Zipser, E. J.: Global distribution of convection penetrating the tropical tropopause, *J. Geophys. Res.*, 110, D23104, doi:10.1029/2005JD006063, 2005.

Monge-Sanz, B. M., Chipperfield, M. P., Simmons, A. J., and Uppala, S. M.: Mean age of air and transport in a CTM: comparison of different ECMWF analyses, *Geophys. Res. Lett.*, 34, L04801, doi:10.1029/2006GL028515, 2007.

Mote, P., Rosenlof, K., McIntyre, M., Carr, E., Gille, J., Holton, J., Kinnersley, J., Pumphrey, H., Russell III, J., and Waters, J.: An atmospheric tape recorder: the imprint of tropical tropopause temperatures on stratospheric water vapor, *J. Geophys. Res.*, 101(D2), 3989–4006, 1996.

Murtagh, D., Frisk, U., Merino, F., et al.: An overview of the Odin atmospheric mission, *Can. J. Phys.*, 80, 309–319, 2002.

**Equatorial transport
as diagnosed from
N₂O variability**

P. Ricaud et al.

[Title Page](#)[Abstract](#)[Introduction](#)[Conclusions](#)[References](#)[Tables](#)[Figures](#)[◀](#)[▶](#)[◀](#)[▶](#)[Back](#)[Close](#)[Full Screen / Esc](#)[Printer-friendly Version](#)[Interactive Discussion](#)

- Naujokat, B.: An updated of the observed quasi-biennial oscillation of the stratospheric winds over the Tropics, *J. Atmos. Sci.*, 43, 1873–1877, 1986.
- O'Sullivan, D. and Dunkerton, T. J.: The influence of the quasi-biennial oscillation on global constituent distributions, *J. Geophys. Res.*, 102, 21731–21743, 1997.
- 5 Randel, W. J., Boville, B. A., Gille, J. C., et al.: Simulation of stratospheric N₂O in the NCAR CCM2: comparison with CLAES data and global budget analysis, *J. Atmos. Sci.*, 51, 2834–2845, 1994.
- Randel, W. J. and Wu, F.: Isolation of the ozone QBO in SAGE II data by singular-value decomposition, *J. Atmos. Sci.*, 53, 2546–2559, 1996.
- 10 Randel, W. J., Park, M., Wu, F., and Livesey, N. J.: A large annual cycle in ozone above the tropical tropopause linked to the Brewer-Dobson circulation, *J. Atmos. Sci.*, 64, 4479–4488, doi:10.1175/2007JAS2409.1, 2007.
- Ricaud, P., Barret, B., Attié, J.-L., et al.: Impact of land convection on troposphere-stratosphere exchange in the tropics, *Atmos. Chem. Phys.*, 7, 5639–5657, 2007, <http://www.atmos-chem-phys.net/7/5639/2007/>.
- 15 Ricaud, P., Attié, J.-L., Teyssèdre, H., El Amraoui, L., Peuch, V.-H., Matricardi, M., and Schlüssel, P.: Equatorial total column of nitrous oxide as measured by IASI on MetOp-A: implications for transport processes, *Atmos. Chem. Phys. Discuss.*, 9, 3243–3264, 2009, <http://www.atmos-chem-phys-discuss.net/9/3243/2009/>.
- 20 Rodgers, C. D.: *Inverse Methods for Atmospheric Sounding: Theory and Practice*, 1st edn., World Sci., River Edge, N. J., 2000.
- Schoeberl, M. R., Douglass, A. R., Newman, P. A., et al.: QBO and annual cycle variations in tropical lower stratosphere trace gases from HALOE and AURA MLS observations, *J. Geophys. Res.*, 113, D05301, doi:10.1029/2007JD008678, 2008.
- 25 Teyssèdre, H., Michou, M., Clark, H. L., et al.: A new tropospheric and stratospheric Chemistry and Transport Model MOCAGE-Climat for multi-year studies: evaluation of the present-day climatology and sensitivity to surface processes, *Atmos. Chem. Phys.*, 7, 5815–5860, 2007, <http://www.atmos-chem-phys.net/7/5815/2007/>.
- Uppala, S. M., Kallberg, P. W., Simmons, A. J., et al.: The ERA-40 re-analysis, *Q. J. Roy. Meteor. Soc.*, 131, 2961–3012 (Part B), 2005.
- 30 Urban, J., Lautié, N., Le Flochmoën, E., et al.: Odin/SMR limb observations of stratospheric trace gases: level 2 processing of ClO, N₂O, HNO₃, and O₃, *J. Geophys. Res.*, 110, D14307, doi:10.1029/2004JD005741, 2005.

Equatorial transport as diagnosed from N₂O variability

P. Ricaud et al.

Table 1. Correlation coefficients between ODIN, SLIMCAT and MOCAGE N₂O and ECMWF zonal wind speed (u) in the Equatorial band (10° S–10° N) from 100 to 1 hPa.

Pressure (hPa)	Correlation Coefficient: N ₂ O vs. u		
	ODIN	SLIMCAT	MOCAGE
100	0.25	0.73	0.17
46	−0.26	−0.23	−0.67
21	−0.60	−0.36	−0.34
10	−0.74	−0.55	−0.55
4.6	−0.62	−0.58	−0.75
2.1	−0.66	−0.58	−0.68
1	−0.71	−0.63	−0.60

Title Page

Abstract

Introduction

Conclusions

References

Tables

Figures

◀

▶

◀

▶

Back

Close

Full Screen / Esc

Printer-friendly Version

Interactive Discussion



Equatorial transport as diagnosed from N₂O variability

P. Ricaud et al.

Table 2. Same as Table 1 but for ECMWF vertical wind (Ω).

Pressure (hPa)	Correlation Coefficient: N ₂ O vs. Ω		
	ODIN	SLIMCAT	MOCAGE
100	0.11	0.69	−0.05
46	0.19	0.31	0.61
21	0.66	−0.05	0.59
10	0.56	0.50	0.59
4.6	0.53	0.22	0.37
2.1	0.56	0.38	0.54
1	0.37	0.37	0.32

Title Page

Abstract

Introduction

Conclusions

References

Tables

Figures

◀

▶

◀

▶

Back

Close

Full Screen / Esc

Printer-friendly Version

Interactive Discussion



Equatorial transport as diagnosed from N₂O variability

P. Ricaud et al.

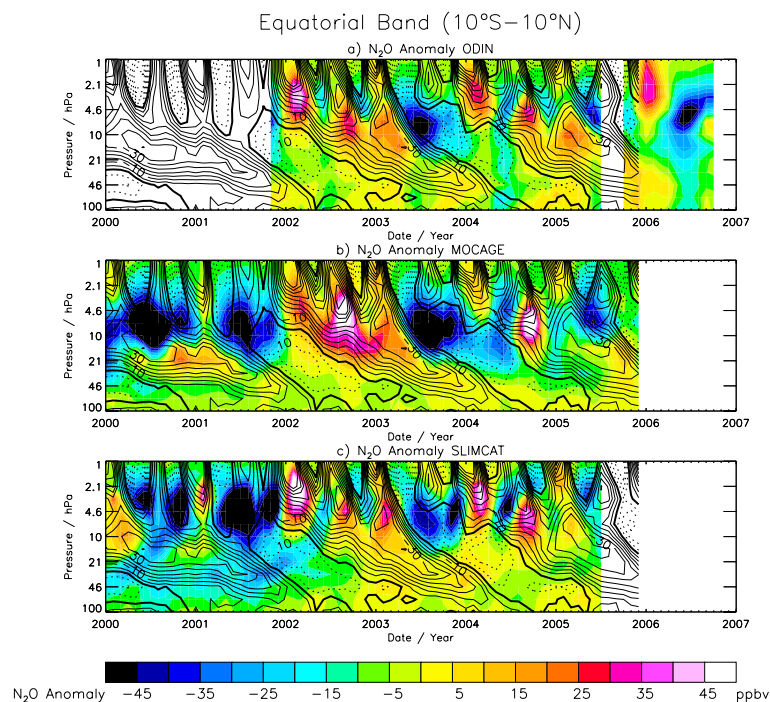


Fig. 1. N₂O anomaly (N₂O minus detrended 2000–2006 average) within 10° S–10° N. From top to bottom: ODIN November 2001–October 2006 (October–November 2005 missing), MOCAGE January 2000–December 2005, and SLIMCAT January 2000–June 2005. Superimposed are the ECMWF zonal winds, Easterlies (Westerlies) in solid (dashed) lines. Intervals are 5 m s⁻¹. The thick solid line represents 0 m s⁻¹.

Title Page

Abstract

Introduction

Conclusions

References

Tables

Figures

◀

▶

◀

▶

Back

Close

Full Screen / Esc

Printer-friendly Version

Interactive Discussion



Equatorial transport as diagnosed from N₂O variability

P. Ricaud et al.

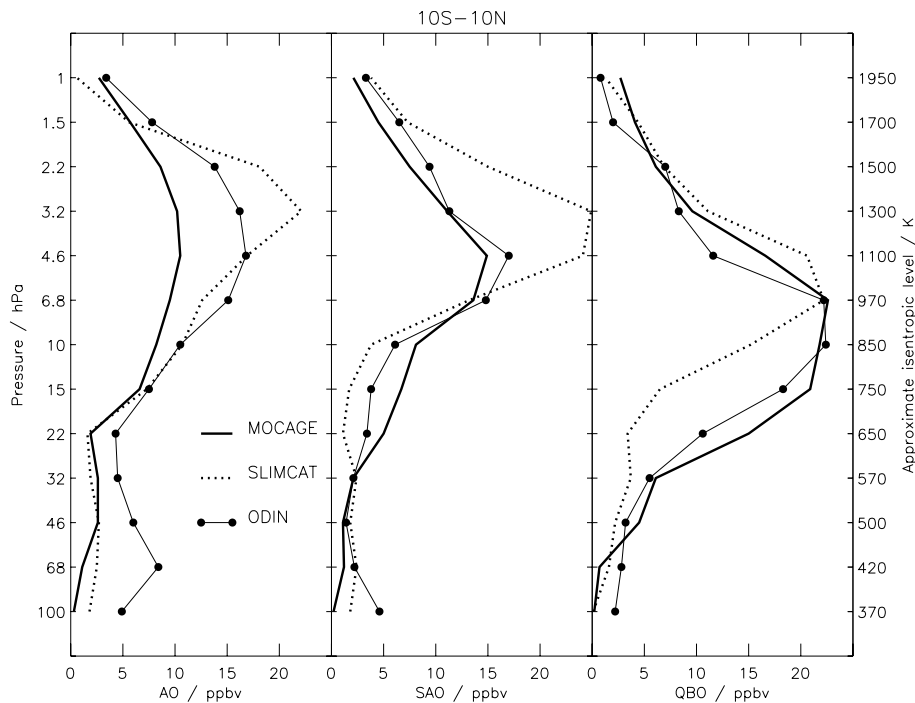


Fig. 2. From left to right: contribution of annual oscillation (AO), semi-annual oscillation (SAO) and quasi-biennial oscillation (QBO) within 10° N–10° S for ODIN (filled circles), SLIMCAT (dashed line) and MOCAGE (solid line).

Title Page

Abstract

Introduction

Conclusions

References

Tables

Figures

◀

▶

◀

▶

Back

Close

Full Screen / Esc

Printer-friendly Version

Interactive Discussion



Equatorial transport
as diagnosed from
 N_2O variability

P. Ricaud et al.

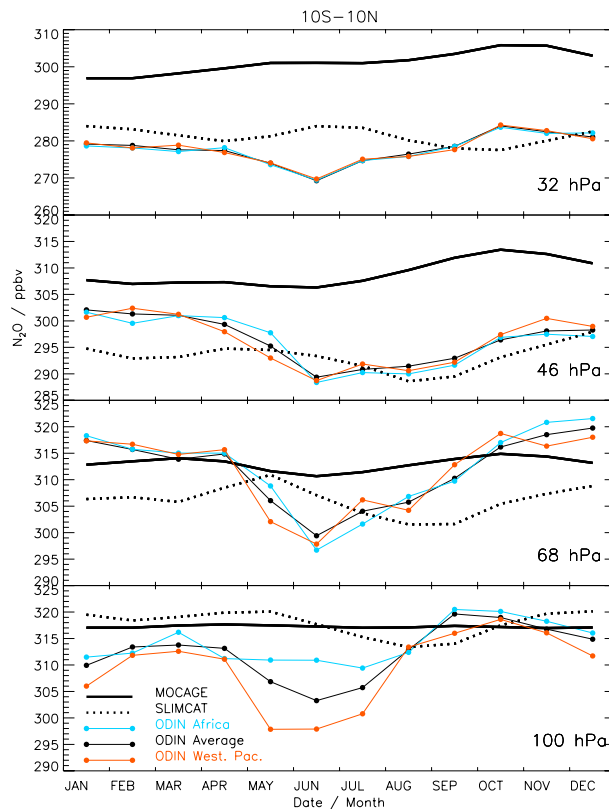


Fig. 3. From bottom to top: N_2O seasonal variations at 100, 68, 47 and 32 hPa within $10^\circ S$ – $10^\circ N$. ODIN zonal mean (black filled circles), over Africa (blue filled circles) and over the Western Pacific (red filled circles), MOCAGE zonal mean (thick solid line) and SLIMCAT zonal mean (dotted line).

[Title Page](#)[Abstract](#)[Introduction](#)[Conclusions](#)[References](#)[Tables](#)[Figures](#)[◀](#)[▶](#)[◀](#)[▶](#)[Back](#)[Close](#)[Full Screen / Esc](#)[Printer-friendly Version](#)[Interactive Discussion](#)

Equatorial transport
as diagnosed from
 N_2O variability

P. Ricaud et al.

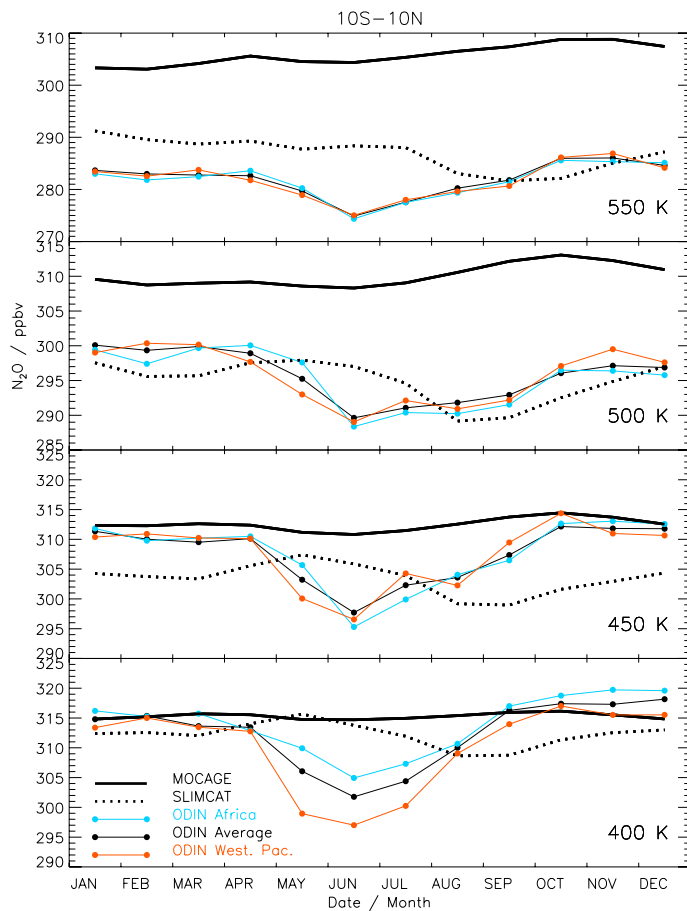


Fig. 4. Same as Fig. 3 but after interpolation on 400, 450, 500 and 550 K isentropic levels.

[Title Page](#)[Abstract](#)[Introduction](#)[Conclusions](#)[References](#)[Tables](#)[Figures](#)[◀](#)[▶](#)[◀](#)[▶](#)[Back](#)[Close](#)[Full Screen / Esc](#)[Printer-friendly Version](#)[Interactive Discussion](#)

Equatorial transport as diagnosed from N₂O variability

P. Ricaud et al.

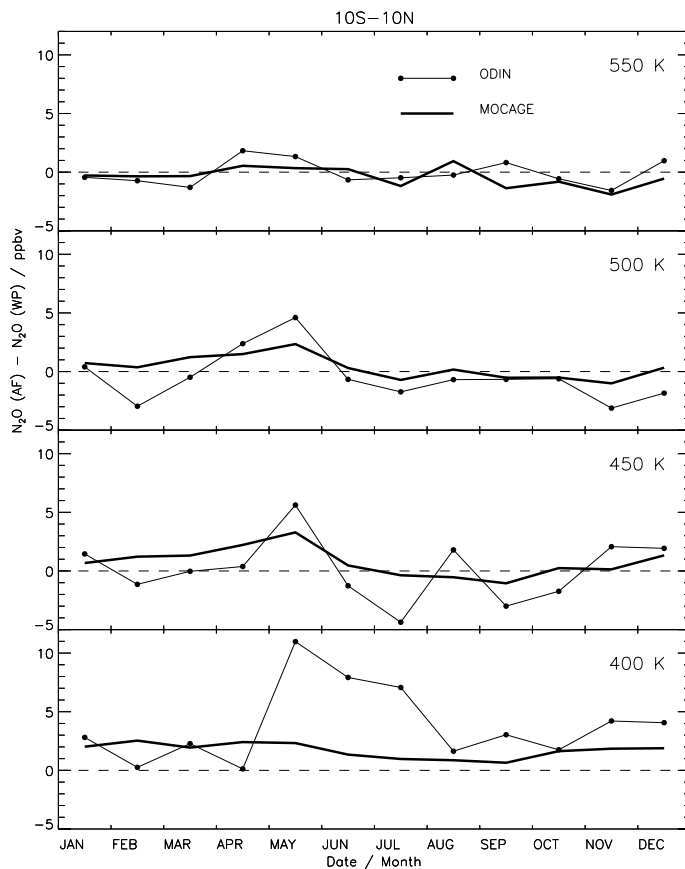


Fig. 5. From bottom to top: N₂O concentration difference (Africa – Western Pacific) at 400, 450, 500 and 550 K. ODIN (black filled circles) and MOCAGE (thick solid line).

Title Page

Abstract

Introduction

Conclusions

References

Tables

Figures

◀

▶

◀

▶

Back

Close

Full Screen / Esc

Printer-friendly Version

Interactive Discussion



Equatorial transport as diagnosed from N_2O variability

P. Ricaud et al.

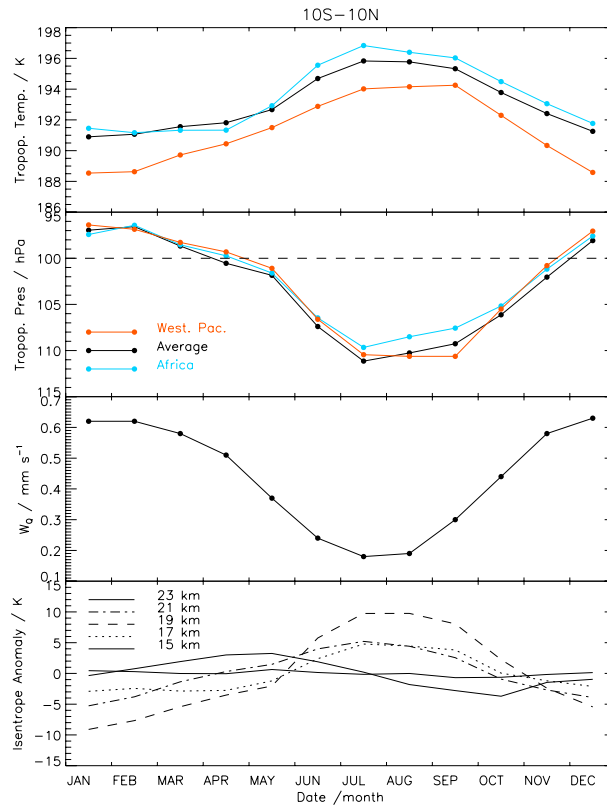


Fig. 6. From top to bottom: NCEP seasonal variation of tropopause temperature, (zonal mean in black, Western Pacific in red, Africa in blue), NCEP tropopause pressure, upwelling calculated from thermodynamic balance (adapted from Randel et al., 2007) and ECMWF potential temperatures between 15 and 23 km.

Title Page

Abstract

Introduction

Conclusions

References

Tables

Figures

◀

▶

◀

▶

Back

Close

Full Screen / Esc

Printer-friendly Version

Interactive Discussion



**Equatorial transport
as diagnosed from
N₂O variability**

P. Ricaud et al.

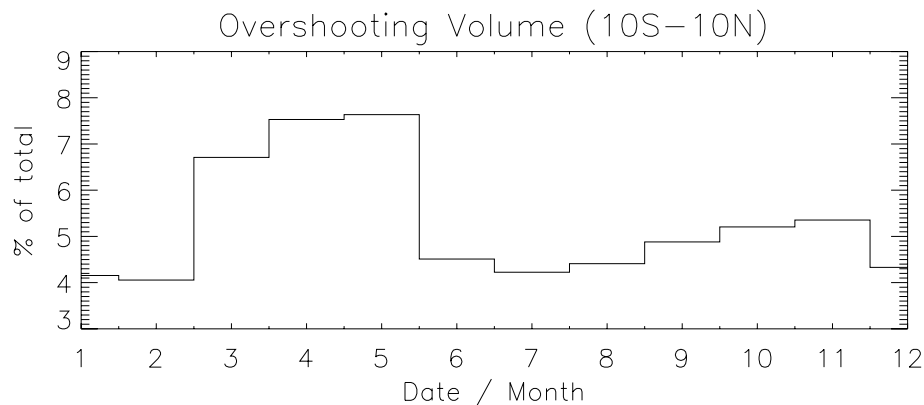


Fig. 7. Seasonal variation of overshooting volume within 10° S–10° N from TRMM Overshooting Precipitation Features (OPFs) above 14 km (in % unit) (adapted from Liu and Zipser, 2005).

[Title Page](#)[Abstract](#)[Introduction](#)[Conclusions](#)[References](#)[Tables](#)[Figures](#)[◀](#)[▶](#)[◀](#)[▶](#)[Back](#)[Close](#)[Full Screen / Esc](#)[Printer-friendly Version](#)[Interactive Discussion](#)

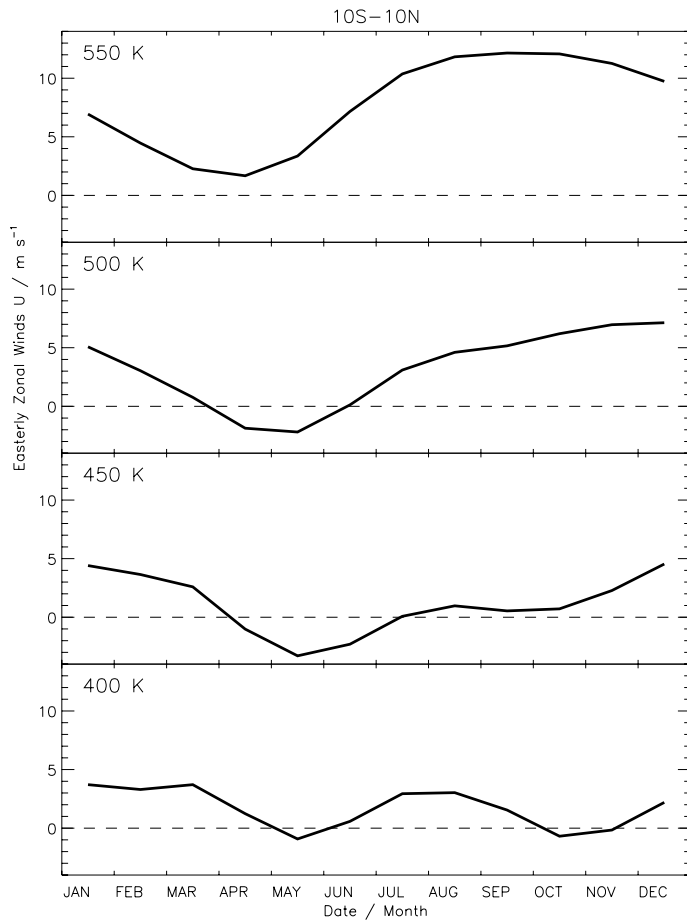


Fig. 8. ECMWF easterly zonal mean wind speed at 400, 450, 500 and 550 K.

**Equatorial transport
as diagnosed from
N₂O variability**

P. Ricaud et al.

Title Page

Abstract

Introduction

Conclusions

References

Tables

Figures

◀

▶

◀

▶

Back

Close

Full Screen / Esc

Printer-friendly Version

Interactive Discussion



Equatorial transport
as diagnosed from
 N_2O variability

P. Ricaud et al.

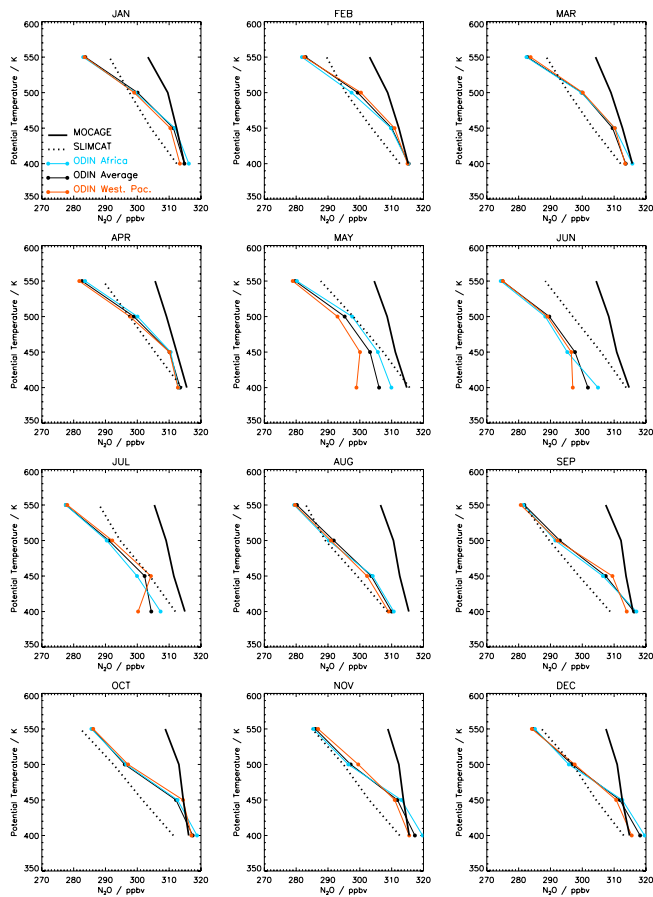


Fig. 9. Monthly mean N_2O vertical profiles from January to December. ODIN zonal mean (black filled circles), over Africa (blue filled circles) and the West Pacific (red filled circles), MOCAGE (thick solid line) and SLIMCAT (dotted line) zonal mean.

[Title Page](#)[Abstract](#)[Introduction](#)[Conclusions](#)[References](#)[Tables](#)[Figures](#)[⏪](#)[⏩](#)[◀](#)[▶](#)[Back](#)[Close](#)[Full Screen / Esc](#)[Printer-friendly Version](#)[Interactive Discussion](#)

Equatorial transport
as diagnosed from
 N_2O variability

P. Ricaud et al.

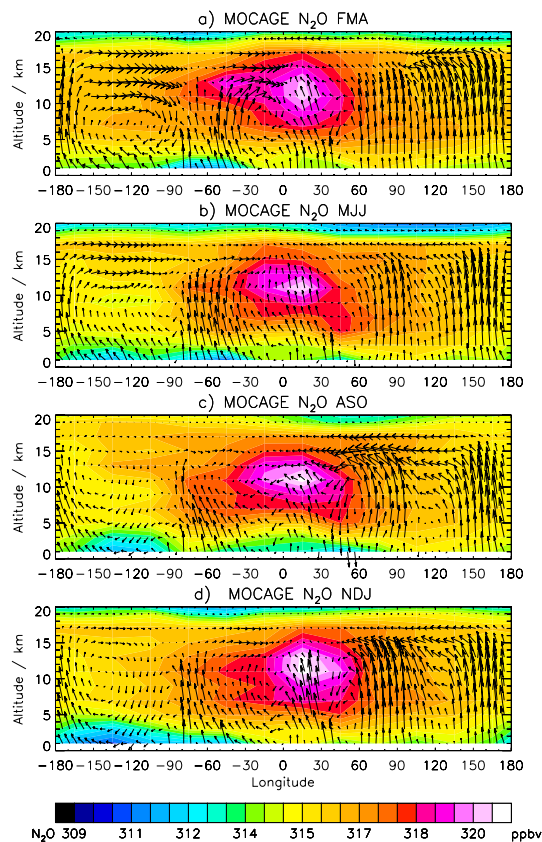


Fig. 10. Mean 2001–2005 MOCAGE N_2O altitude-longitude cross-section within 10° S– 10° N. From top to bottom: FMA, MJJ, ASO and NDJ. Superimposed are the wind direction and speed where the vertical component is amplified by a factor 100.

[Title Page](#)[Abstract](#)[Introduction](#)[Conclusions](#)[References](#)[Tables](#)[Figures](#)[◀](#)[▶](#)[◀](#)[▶](#)[Back](#)[Close](#)[Full Screen / Esc](#)[Printer-friendly Version](#)[Interactive Discussion](#)